Available online at www.sciencedirect.com

ScienceDirect

Procedia Materials Science 5 (2014) 780 – 786

Procedia Materials Science

www.elsevier.com/locate/procedia

International Conference on Advances in Manufacturing and Materials Engineering, AMME 2014

Structural and Electrical Properties of Aluminium Substituted Nano Calcium Ferrites

*Ch.Mamatha[a],M. Krishnaiah[a], C. S. Prakash[b], Kishor G. Rewatkar[c]

[a]*Department of Physics, Sri Venkateswara University, Tirupathi, Andhra Pradesh, India*
[b]*Department of Physics, SJCIT, Chickkaballapur, Karnataka, India.*
[c]*Department of Physics, Dr. AmbedkarScience College, Nagpur, Maharashtra, India*
Email: mamathasree@yahoo.co.in

Abstract

Substituted M-type Hexaferrites are ferrimagneticmaterials, which are hard ferrites. In the current study, Aluminum substituted Hexaferrite samples, with composition $CaFe_{12-x}Al_xO_{19}$ (x=3,x=4), have been prepared by Solution combustion synthesis using Metal Nitrates. The powders were characterized with XRD, TEM, SEM, and EDS. XRD analysis indicated the formation of single-phase substituted M-type calcium hexaferrites with space group of $P6_3/mmc$ (194). Electrical properties were studied with the help of LCR Meter. Variations of dielectric constant, dielectric modulus, DC conductivity, AC conductivity etc. of bulk samples have been investigated as a function of frequency and temperature. Activation energies were calculated at both ferrimagnetic and paramagnetic regions. The enhanced resistivity of aluminum doped calcium hexaferrite is a prospective application in microwave devices.

*Keywords:*hexaferrites; combustion; dielectric constant; Activation Energy.

* Corresponding author. Tel.: +919972008585; fax: +0-000-000-0000 .
E-mail address: mamathasree@yahoo.co.in

2211-8128 © 2014 Elsevier Ltd. This is an open access article under the CC BY-NC-ND license (http://creativecommons.org/licenses/by-nc-nd/3.0/).
Selection and peer-review under responsibility of Organizing Committee of AMME 2014
doi:10.1016/j.mspro.2014.07.328

1. Introduction

Ferrites are large family of oxides with remarkable electrical and magnetic properties. Their large applications as permanent magnets are based on the very basic properties of ferrites, a significant saturation magnetization, a high electrical resistivity, low electrical losses, very good chemical stability and low cost [C.S.Prakash and D.K.Kulkarni]. The possibility of preparing ferrites in the form of Nano particles has opened a new and exciting trend in the research field [Rau ́l Valenzuela, 2012]

Substituted hexaferrites belong to M-Type with general formula $MFe_{12}O_{19}$ where M is usually barium, strontium, Calcium or Lead. The basic structure consists of 38 oxygen and 24 ferric ions. All ferric ions occupy five different lattice sites in the unit cell such as 2a, 4f2 and 12k, which are octahedral sites, 4f1, tetrahedral site and 2b, bi-pyramidal site [C.S.Prakash, 1994]. When doped with other trivalent metal ions, the properties of the calcium ferrites would get altered.

There are many methods for synthesis of Hexagonal ferrite nanoparticles, like chemical co-precipitation [Wang etal 2002], hydrothermal [Junliang 2010], sol-gel [J.Huang etal 2003], combustion [Robert C.Puller 2012] etc. In the present work, Calcium hexaferrites doped with trivalent Al ions synthesized by combustion method are studied and reported.

2. Experimental

2.1. Synthesis techniques

Two samples of M-type aluminium substituted calcium hexaferrites with general formula $CaAl_xFe_{12-x}O_{19}$ (x=3,4) have been synthesized successfully by solution combustion to study the structural and electrical properties. Samples were prepared with AR grade calcium nitrate $Ca(NO_3)_2$ $4H_2O$, iron nitrate $Fe(NO_3)_3$ $9H_2O$, aluminium nitrate $Al(NO_3)_3$ $9H_2O$ and freshly prepared Oxalyl dihydrazideODH ($C_2H_6N_4O_2$) was used as fuel [P.Lubitzetal 1980]. In Solution combustion method, the stoichiometric amounts of metal nitrates which act as an oxidizing agent and fuel (Oxalyldihydrazide (ODH) [C2H6N4O2]) acts as a reducing agent with exothermic reaction. The maximum heat is released when oxidizer to fuel ratio (O/F) becomes equal to unity. Stoichiometric amount of metal nitrates along with ODH were dissolved completely in double distilled water to form an aqueous solution. After continuous stirring for about 20 min., with the help of magnetic stirrer, the solution was kept in the preheated muffle furnace at 300°C. Initially the solution boils and undergoes dehydration followed by decomposition.Within few minutes and after reaching spontaneous combustion, the solution ignites like smouldering with the evolution of a large volume of gases (N_2 and CO_2) It releases large amount of heat vaporizing all the solution to become a solid at 430^{o}C. Prepared powders are loose, Foamy, pores, and highly friable. Samples were calcinated at 900°C for 3 hours and allowed to cool gradually.

2.2. Structural studies

The structural characterization of the samples was performed by PAN analytical X'pert Pro diffractometer with Cu-Kα radiation (λ=1.5405Å) in the 2θ range of 10-80, in angular steps of 0.02°. The average particle size, D, was determined from line broadening of (107) reflection using Scherrer formula,

$$D = \frac{k\lambda}{\beta \cos\theta} \quad (1)$$

Where β is the angular line width at half maximum intensity and θ the Bragg angle for that peak, k is predetermined constant and λ is the wavelength of the x-ray.

Values of lattice constants ‘a’, ‘c’, and the unit cell volume ‘V_{cell}’ were calculated by taking hkl parameters and distance between the planes (d), using following equations.

$$\frac{1}{d^2} = \frac{4(h^2 + k^2 + hk)}{3a^2} + \frac{l^2}{c^2} \tag{2}$$

$$V_{cell} = 0.866 a^2 c \tag{3}$$

The morphology and compositional analysis were studied using SEM and Energy Dispersive Spectroscopy (EDS) attached with SEM and reported earlier in the conference. The particle size of each sample was examined by Transmission Electron Microscope (TEM)

2.3 *Electrical and dielectric studies*

Dielectric measurements were carried out at room temperature using LCR meter over a wide frequency range from 100 Hz up to 1 MHz.The dielectric constant (ε′) and dielectric loss (ε′′) were calculated using the following formulae.

$$\varepsilon' = \frac{cd}{\varepsilon_0 A} \tag{4}$$

$$\varepsilon'' = \varepsilon' \tan\delta \tag{5}$$

Where ‘c’ is the capacitance, ‘d’ is thickness of the sample, ‘A’ is the area of cross section and ε_0 is permittivity of free space.

The AC conductivity measurements were recorded out in the range of frequencies 100Hz-1MHz. at room temperature and DC measurements were recorded in the range of temperatures 310k – 650K. Activation energies are calculated in both paramagnetic and ferrimagnetic regions.

3. Results and Discussions

3.1 Structural analysis

Figure 1 shows the XRD pattern of the samples. X-ray diffraction studies confirm the formation of hexaferrites with the space group $P6_3/mmc$. The intensity diffraction peaks of samples have been found at (006), (107), (202), (109), (214) etc. orientations as mentioned in the figure 1. The highest intensity diffraction peaks of samples have been found at 2θ=33.37°(for $CaAl_3Fe_9O_{19}$) and 33.46°(for $CaAl_4Fe_8O_{19}$) with (107), orientation. Due to the small ionic radius of Al^{+3} ion (0.53Å) than Fe^{+3} ion (0.67 Å), the lattice parameters ‘a’, ‘c’ and volume of the cell shows slight variation with substitution of Al^{+3} ions (Table 1). Figures 2a and 2b show TEM photographs of samples. TEM pictures confirm that the particles are in Nano size and cylindrical shape.

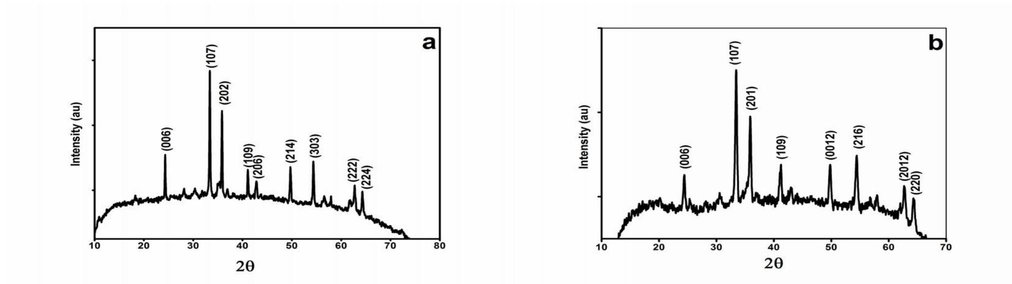

Figure 1: XRD spectrum of (a) $CaAl_3Fe_9O_{19}$ (b) $CaAl_4Fe_8O_{19}$

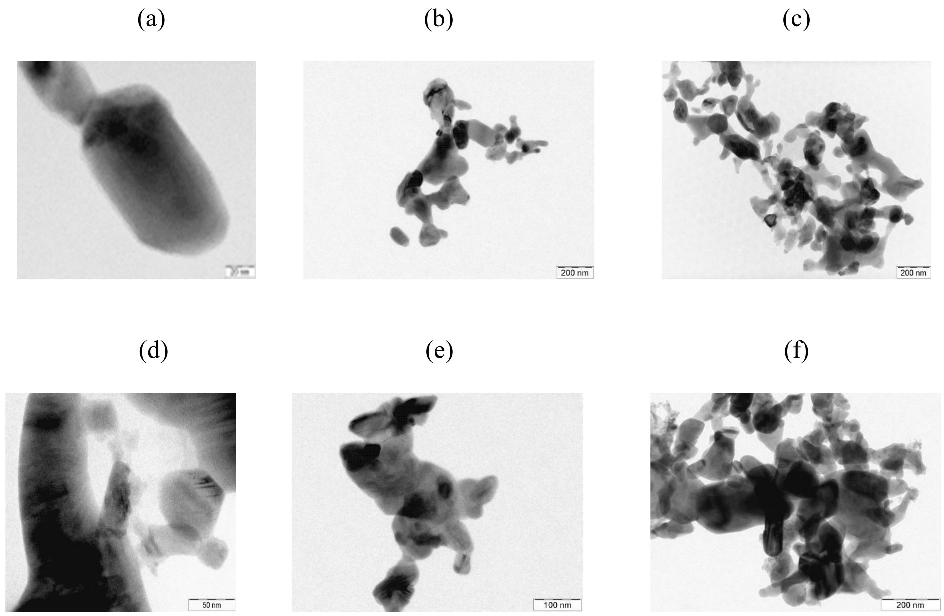

Figure 2: TEM pictures of (a,b,c) $CaAl_3Fe_9O_{19}$ (d,e,f) $CaAl_4Fe_8O_{19}$

3.2 Dielectric properties

The variation of real and imaginary parts of dielectric constant and dielectric loss as a function of frequency are shown in Figures (3a and 3b). The value of dielectric constant (ε') rapidly decreases with increasing frequency up to 10^5 Hz. Values are almost constant at higher frequencies. The Dielectric loss (ε'') values rapidly decrease with increasing frequency. However the values decrease with Al^{+3}content.

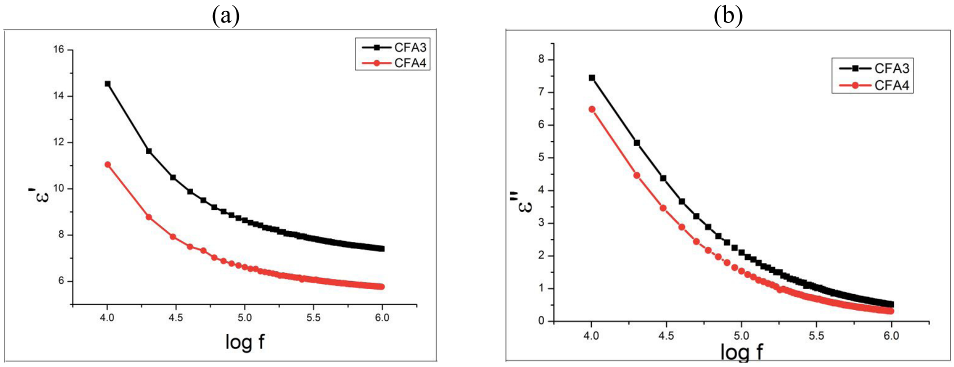

Figure 3: Variation of (a) dielectric constant (b) Dielectric loss with frequency

Figs. 4(a) and (b) show the variations in the imaginary part of the complex modulus with frequency for both samples. From the figure it is evident that the variation is same for both samples, but high values for more Al content. The peak value of M'' increases with increasing Al ions. At higher frequencies M'' values are almost same for both samples. The value of dielectric loss tangent (tan δ) depends on various factors such as composition, stoichiometry, dopant, synthesis method, and sintering temperature of the pellets. Figure 5 shows the variation of loss tangent with temperature.

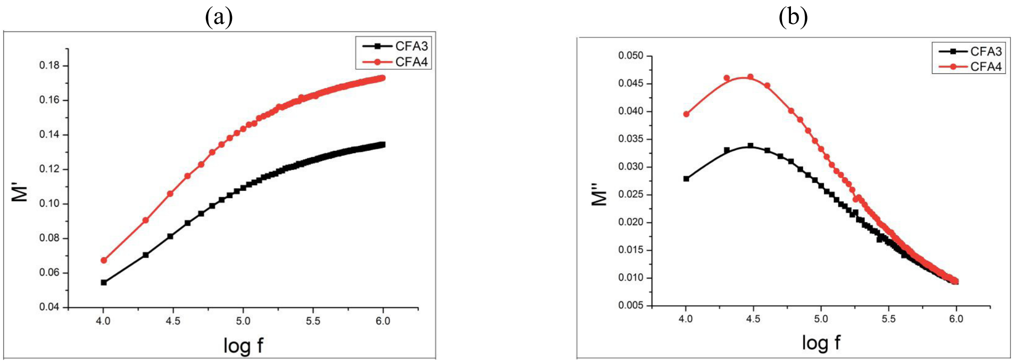

Figure 4: Variation of (a) real and (b) imaginary parts of dielectric modulus with frequency

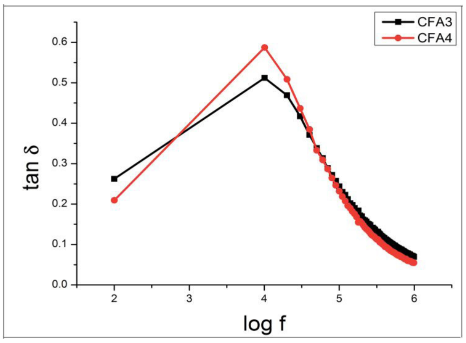

Figure 5: variation of loss tangent with frequency

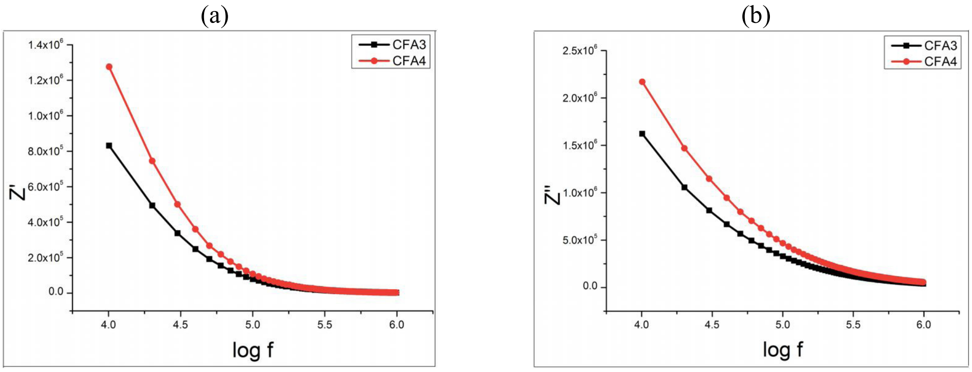

Figure 6: Variation of (a) real and (b) imaginary parts of Impedance with frequency

Figure 6 (a and b) show the variation of complex impedance (Z’ and Z’’) with frequency. Impedance decreases with Aluminium content at low frequencies, but almost remains same for both the samples at high frequencies.

3.4 AC conductivity

Figure 7 (a) shows the variation of conductivity with frequency. Ac conductivity variation is almost linear. As the frequency is increased, hopping of carriers also increases, thereby increasing the conductivity. Conductivity decreased with increase in Aluminium ions.

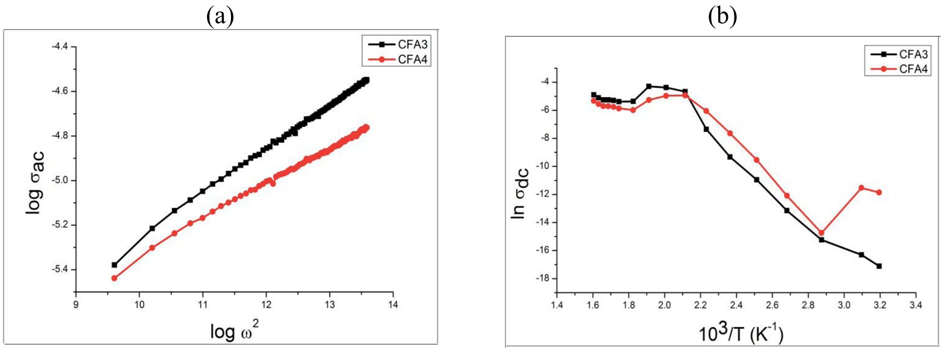

Figure 7: The plot of (a) log ω^2 vs log σ_{ac} (b) $10^3/T$ vs ln σ_{dc}

3.3 DC conductivity properties

The DC Conductivity of the material increases with increase in Temperature. The relation between electrical conductivity and temperature is given by

$$\sigma = \sigma_0 \exp(-E_a / KT) \tag{6}$$

Where, T is absolute temperature, k is Boltzmann’s constant and E_a is the activation energy that is the energy needed to release an electron from the ion for a jump to neighbouring ion, giving rise to the electrical conductivity. The activation energies are calculated from the slope of the plot (figure 7b) and the values are tabulated. Activation energies increase with Al^{+3} content. The kink in the graph shows the transition. At room temperature both the samples are ferrimagnetic. As temperature is increased, transition takes place and at high temperature they become paramagnetic. Transition temperatures are found and tabulated.(table 1). In Ferrimagnetic region, the conductivity increases with increase in Aluminium content, where as it decreases in paramagnetic region.

Table 1: calculated structural and electrical parameters

Compound	Crystallite size (nm)	Lattice parameters (Å)		Volume of the cell V (Å^3)	Transition Temperature T (K)	Resistivity At RT σ (MΩcm)	Activation Energy ΔE (ev)	
		'a'	'c'				Para	Ferri
$CaFe_9Al_3O_{19}$ (CFA3)	30.8	5.980	21.799	675.55	515	17.017	0.09	0.98
$CaFe_8Al_4O_{19}$ (CFA4)	23.4	5.793	21.967	638.85	482	28.189	0.18	1.2

4. Conclusion

Single phase M-type Aluminium substituted calcium hexaferrite samples synthesized by Solution Combustion Technique were examined. With the analysis of XRD pattern it has been confirmed that the structure is Hexagonal with space group $P6_3$/mmc. TEM images confirmed that they are Nano particles. Dc electrical conductivity, activation energies showed a gradual increase with increase in the content of Al ions at room temperature. An improvement in the grain size is observed for the samples than the earlier reported about 90 nm [Sanjay Gawalietal 2012], where the samples were prepared by the Sol-gel and auto-combustion methods.

References

C.S.Prakash andD.K.Kulkarni 1994, Chromium substituted hexagonal calcium ferritesInd Pure Appl Physics. 32361

C.S.Prakash and D.K.Kulkarni 2012Variational Effect in Substituted Calcium Hexaferrite , International Journal of Knowledge Engineering. Vol 3, Issue 1, 79-80

C.S.Prakash, V.M.Nanoti, G.M.Rao and D.K.Kulkarni. 1995, Substitutional effect of magnetic behavior of calcium hexaferrite.J.Magn. Magn. Mater .140-144 , 2089-2090.

C.S.Prakash. V.M.Nanoti and D.K.Kulkarni, 1995 Magnetic Characterization of calcium hexaferritesMaterials Letters, 24 171.-173

Ch.Mamatha, M.Krishnaiah and C.S.Prakash, 2013, Comparative Study of $CaAl_3Fe_9O_{19}$ and $CaAl_4Fe_8O_{19}$ Nanoparticles Synthesized by Solution Combustion Method. Proceedings of the Second National Seminar on New Materials Research and Nanotechnology OOTY, 135-138. (ISBN No.978-93-81104-33-0)

D.K.Kulkarni and C.S.Prakash, 1994, Structural and magnetic study of $CaAl_4Fe_8O_{19}$ Bull.Mater.Sci. 17, p.35-39.

K.G. Rewatker, C.S.Prakashand D.K.Kulkarni. 1997, Synthesis and characterization of $CaAl_x(CuTi)_{6-x}O_{19}$hexaferrite system. Materials Letters, 28 ,365-368.

Rau´l Valenzuela , 2012, Novel Applications of Ferrites, Physics Research International, Article ID 591839 9 pages doi:10.1155/2012/591839

RobertC.Pullar, 2012, Hexagonal Ferrites: A Review of the synthesis, properties and applications of haxaferrite ceramics. Progress in Materials Science, 57, 1191–1334.

Sanjay R. Gawali, Kishor G. Rewatkar and Vivek M. Nanoti, 2012, Structural and Electrical properties of M-type Nanocrystalline Aluminium substituted Calcium Hexaferrites Advances in Applied Science Research, 3 (5):2672-2678